Frustration-Induced Superconductivity in the t-t' Hubbard Model

Changkai Zhang (张昌凯),[1] Jheng-Wei Li,[2] Dimitra Nikolaidou,[1] and Jan von Delft[1]
[1]Arnold Sommerfeld Center for Theoretical Physics, Ludwig-Maximilians-Universität München, 80333 Munich, Germany
[2]Université Grenoble Alpes, CEA, Grenoble INP, IRIG, Pheliqs, F-38000 Grenoble, France

(Received 22 August 2023; revised 5 December 2024; accepted 24 February 2025; published 18 March 2025)

The two-dimensional Hubbard model is widely believed to capture key ingredients of high-T_c superconductivity in cuprate materials. However, compelling evidence remains elusive. In particular, various magnetic orders may emerge as strong competitors of superconducting orders. Here, we study the ground state properties of the doped two-dimensional t-t' Hubbard model on a square lattice via the infinite projected entangled-pair state method with U(1) or SU(2) spin symmetry. The former is compatible with antiferromagnetic orders, while the latter forbids them. Therefore, we obtain by comparison a detailed understanding of the magnetic impact on superconductivity. Moreover, an additional t' term accommodates the particle-hole asymmetry, which facilitates studies on the discrepancies between electron- and hole-doped systems. We demonstrate that (i) a positive t'/t significantly amplifies the strength of superconducting orders; (ii) at sufficiently large doping levels, the t-t' Hubbard model favors a uniform state with superconducting orders instead of stripe states with charge and spin modulations; and (iii) the enhancement of magnetic frustration, by increasing either the strength of next-nearest neighbor interactions or the charge doping, impairs stripe orders and helps stabilize superconductivity.

DOI: 10.1103/PhysRevLett.134.116502

Introduction—Despite continuous efforts during the past few decades, the physics of high-T_c superconductivity in cuprate materials [1] remains unclear [2,3]. The two-dimensional (2D) Hubbard model [4] on a square lattice is believed to capture the essential low-energy features of cuprates. Various numerical methods [5–10] have been used to tackle this issue. Nevertheless, previous computational attempts generate numerous candidate ground states [11,12] very close in energies with abundant combinations of charge and spin orders. Experiments [13–20] also confirm simultaneous charge and spin modulated states coexisting or competing with superconductivity. This triggers our curiosity on the interplay between the antiferromagnetic (AFM) background and the high-T_c superconductivity in cuprates.

Typical candidates encompass a uniform state [21–38] and various stripe states [11,33,39–52]. The former features a uniform charge density and is commonly associated with d-wave superconductivity, while the latter often exhibit charge-density and spin-density waves with diverse periods, with only part of them displaying coexisting superconductivity. For the nearest neighbor (NN) minimal Hubbard model, a series of advanced numerical methods reached a consensus [11] that the ground state at $1/8$ hole doping is a filled (one hole per unit cell of the charge order) period 8 stripe state devoid of superconducting orders. The half-filled period 4 stripe state [13,20,53] favored more in, e.g., LaSrCuO materials emerges primarily with negative next-nearest neighbor (NNN) hopping, as demonstrated in numerous computational simulations [48,51,54–59]. This motivates our investigations beyond the minimal Hubbard model.

Concurrently, multiple recent studies [60–62] focusing on the extended t-J model have uncovered substantially more robust superconducting orders in electron-doped settings as opposed to hole-doped configurations, a finding that contradicts experimental observations. Explorations of the extended Hubbard model using the density matrix renormalization group have yielded inconsistent outcomes [63,64], further underscoring the significance of research beyond the minimal Hubbard model.

In this Letter, we use the infinite projected entangled-pair state (iPEPS) [9,10] ansatz and simple update algorithm [65] to study the ground state properties of the t-t' Hubbard model. Our iPEPS ansatz is less susceptible to finite-size effects than the density matrix renormalization group on cylinders. Leveraging our cutting-edge QSpace tensor library [66,67], we are capable of conducting simulations with U(1) or SU(2) spin symmetry, where the former admits local magnetic moments and the latter forbids them. This allows us to scrutinize the impact of magnetic orders on pairing properties. Our simulations demonstrate that (i) a positive t'/t significantly amplifies the strength of

superconducting orders; (ii) at sufficiently large doping, the t-t' Hubbard model favors an SU(2) uniform state with d-wave pairing orders instead of a U(1) stripe state in [51]; and (iii) the enhancement of magnetic frustration, by increasing either the strength of NNN interactions or the charge doping, impairs stripe orders and helps stabilize superconductivity.

Model—The 2D t-t' Hubbard model on a square lattice is defined via the following Hamiltonian:

$$\mathcal{H} = -\sum_{i,j,\sigma} t_{ij}[c^{\dagger}_{i\sigma}c_{j\sigma} + \text{H.c.}] + U\sum_{i} n_{i\uparrow}n_{i\downarrow}. \qquad (1)$$

Here, $t_{ij} = t$ or t' for NN or NNN, respectively, and zero otherwise; U measures the on-site Coulomb repulsion. Throughout this Letter, we use $U/t = 10$, as established to be realistic for cuprate materials [68,69], and set $t = 1$ for convenience.

Method—In our computations, we apply the fermionic iPEPS [70–77] ansatz, a tensor network method targeting 2D lattice models, to simulate the t-t' Hubbard model in the thermodynamic limit. The ansatz exploits translational symmetry by assuming that the infinite tensor network consists of periodically repeated supercells of tensors. Each supercell comprises several rank-5 tensors with one physical index carrying states in the local Hilbert space, and four auxiliary indices connecting neighboring sites. The accuracy of the simulation can be controlled by the bond dimensions of the auxiliary indices. Different supercell sizes yield stripe states with different periods in charge or spin orders. Previous research [51,60,63] on the Hubbard model or the t-J model has identified stripe states with period 4 charge orders as a representative stripe state. Therefore, we hereby focus on the period 4 stripe state. Further discussions and details regarding stripes with longer periods can be found in Supplemental Material [78].

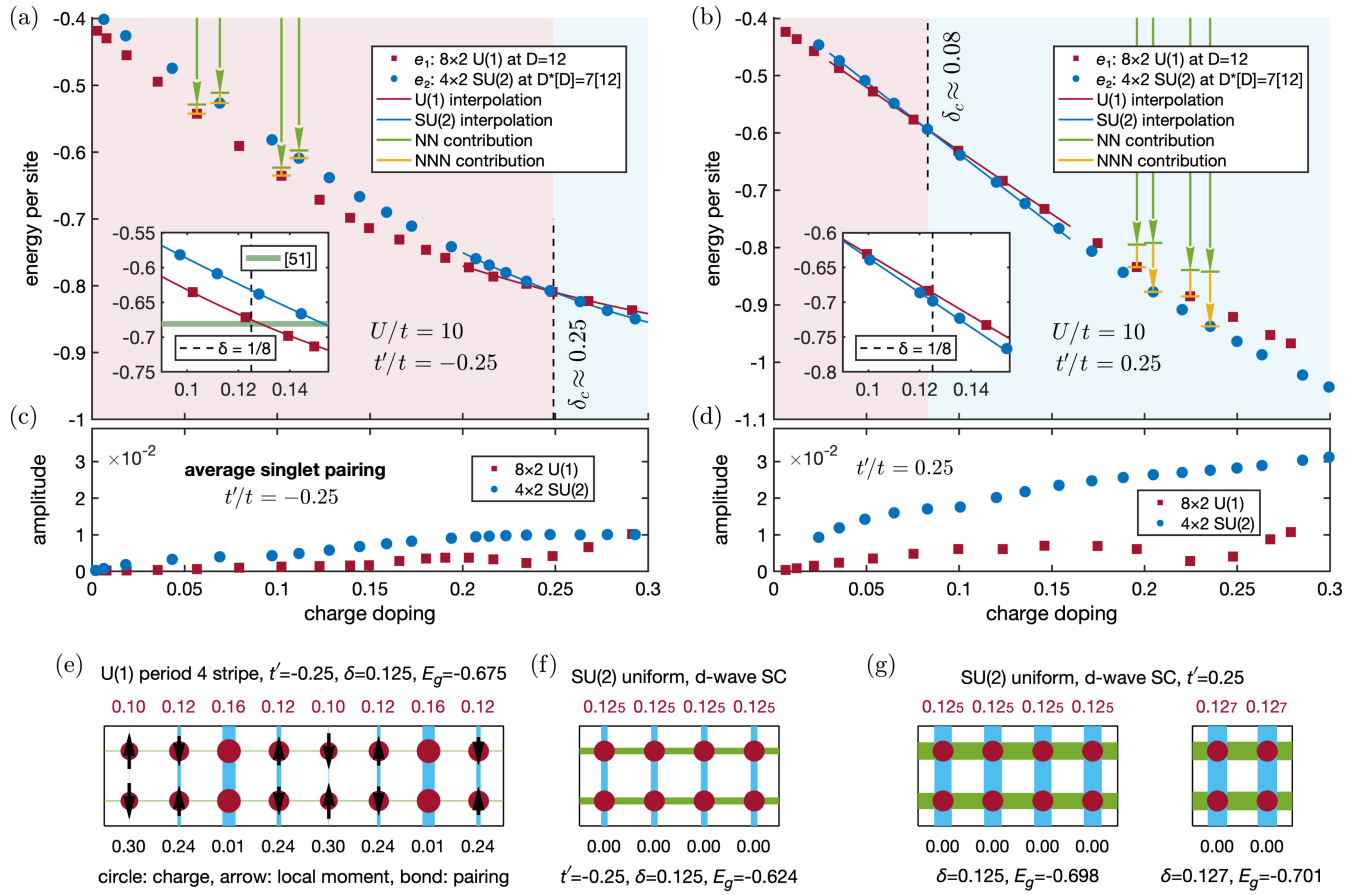

FIG. 1. The ground state energy per site (a), (b) and singlet pairing (c), (d) vs doping δ of the t-t' Hubbard model at $U/t = 10$ and (a), (c) $t'/t = -0.25$ or (b), (d) $t'/t = 0.25$, computed via U(1) iPEPS (red squares) on an 8×2 supercell at bond dimension $D = 12$ and SU(2) iPEPS (blue circles) on a 4×2 supercell keeping $D^* = 7$ multiplets (bond dimension $D = 12$). Green and yellow arrows, respectively, indicate the NN (including on site) and NNN contributions to the energy for several typical data points. Inset: enlargement of the region near $1/8$ doping. (e)–(g) Details of the U(1) and SU(2) symmetric ground states on 8×2, 4×2, and 2×2 supercells. Radii of red circles and lengths of black arrows are proportional to the charge density (top rows) and the local moments (bottom rows), respectively. Bond widths indicate NN singlet pairing amplitudes and two different colors indicate opposite signs. For (f), (g), we used $D^*[D] = 8[13]$ for reasons explained in Supplemental Material [78].

The optimization is performed via imaginary time evolution [79] in which projector $\exp\{-\tau(\mathcal{H}-\mu N)\}$ (τ is a small number, $\mathcal{H}$ the Hamiltonian, μ the chemical potential, and N the charge density) is repeatedly applied to some random initial state until the ground state energy converges. Models with NNN interactions are computationally very expensive. Therefore, we choose the simple update scheme [65,70,71] for a balance between accuracy and computational complexity. Observables are extracted by contracting the tensor network using the corner transfer matrix method [70,72,80–83]. The QSpace tensor library [66,67,84] is used to implement either U(1) or SU(2) spin symmetry.

The U(1) iPEPS simulations are conducted on an 8×2 supercell at bond dimension $D = 12$. This is required for capturing the period 4 charge orders, as the corresponding spin order periods are typically twice as long as the charge periods. The SU(2) iPEPS simulations are performed on a 4×2 or 2×2 supercell by keeping $D^* = 7$ symmetry multiplets (corresponding to a bond dimension $D = 12$) [66]. Spin orders are suppressed upon enforcing SU(2) symmetry, making a 4×2 supercell adequate to detect any potential period 4 orders, while the 2×2 supercell is employed to ascertain the uniformity of the ground state. Charge doping is adjusted by tuning the chemical potential.

Energetics—Figures 1(a) and 1(b) show the ground state energy per site of the t-t' Hubbard model as a function of doping under $U/t = 10$ and $t'/t = \mp 0.25$, computed via the U(1) and SU(2) iPEPS and denoted as e_1 (red) and e_2 (blue), respectively. Figures 1(c) and 1(d) show the corresponding singlet pairing amplitudes. Figures 1(e) and 1(f) display, respectively, the detailed characteristics of the U(1) and SU(2) ground states with a negative t'/t at the predominantly studied $1/8$ doping. Figure 1(g) presents SU(2) ground states with a positive t'/t, showcasing numerically significant d-wave singlet pairing orders.

Utilizing an 8×2 supercell, our U(1) iPEPS generates a nonsuperconducting stripe state with a period 4 charge-density wave and a period 8 antiferromagnetically ordered spin-density wave. These attributes, along with the ground state energy acquired, are generally consistent with the findings in [51]. By contrast, when we enforce the SU(2) symmetry and suppress spin orders, we find a uniform state without any charge orders, at odds with finite-size studies [56,60,63]. Moreover, strong d-wave pairing emerges for positive t'/t, which implies superconductivity. The SU(2) iPEPS on 4×2 and 2×2 supercells produces physically identical states, confirming the uniformity of the ground state.

Near zero doping, we find $e_2 > e_1$. This is consistent with the well-established fact that the Heisenberg model on a square lattice has an AFM ground state that breaks SU(2) symmetry. However, as the doping increases, e_2 decreases faster than e_1. They intersect at $\delta_c \approx 0.25$ for $t'/t = -0.25$ and $\delta_c \approx 0.08$ for $t'/t = 0.25$ (first order transition), as depicted in Figs. 1(a) and 1(b), in agreement with prior observations [51] that a negative or positive t'/t favors stripe or uniform states, respectively. Intuitively, a positive t'/t promotes diagonal hopping of the doped charges, which in turn disrupts the AFM background in the vicinity of the domain wall within the stripe states, rendering the presence of domain walls less desirable [45].

The lower energy of the SU(2) relative to the U(1) ground state at large doping can be understood as the result of magnetic frustration induced by the NNN hoppings. The U(1) stripe state still accommodates AFM orders and thus suffers strongly from magnetic frustrations with NNN hopping. By contrast, the SU(2) uniform state is less frustrated since it hosts no local spin orders. Indeed, the NNN terms contribute much less to lowering the energy e_1 of the stripe state than to the energy e_2 of the uniform state, as indicated via the yellow arrows in Figs. 1(a) and 2(b).

This issue is further elaborated in Figs. 2(a) and 2(b), showing the contribution of NN (including on site) and NNN terms to the total energy per site as a function of doping, respectively. Throughout the entire doping range in

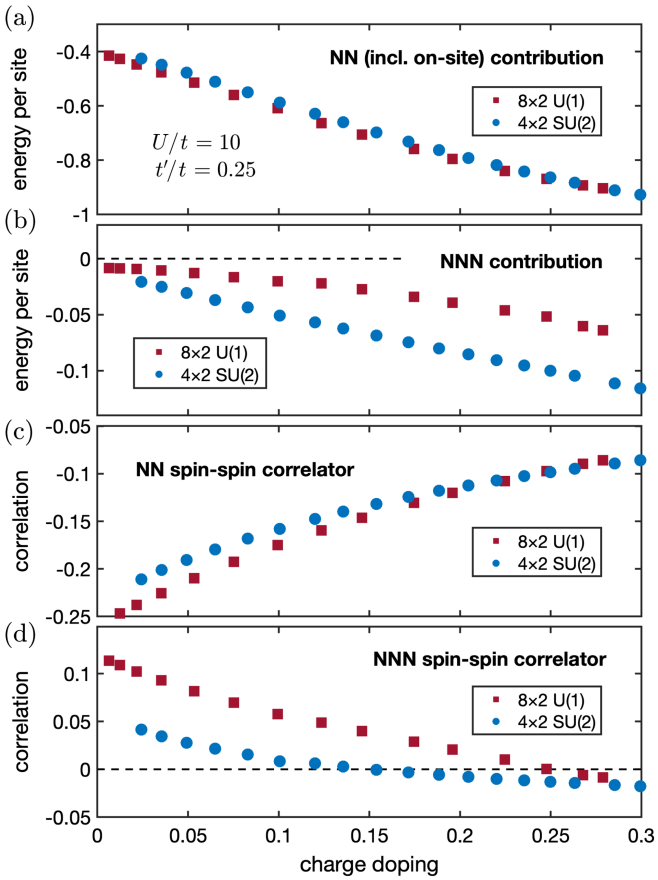

FIG. 2. The contribution of (a) the NN (including on site) and (b) the NNN terms to the total energy per site in the U(1) and SU(2) ground states, respectively, as a function of doping. (c) The NN and (d) NNN spin-spin correlators in the U(1) and SU(2) ground states, respectively.

our study, the NN contribution is marginally lower in the U(1) states than in the SU(2) states. Conversely, the NNN contribution is substantially lower in the SU(2) than the U(1) cases, ultimately leading to a lower overall energy for the SU(2) states at large doping levels. As a comparison, Figs. 2(c) and 2(d) show the NN and NNN spin-spin correlators, respectively. The NN correlations stay negative for both the U(1) and SU(2) states, reflecting the overall AFM background. The NNN correlations, however, turn negative considerably sooner for the SU(2) states than for the U(1) states, echoing the findings in ultracold atom experiments that doped charges drive the NNN spin-spin correlation negative [85–89]. This indicates that the SU(2) state better reconciles the magnetic frustration, thereby achieving a lower NNN energy. Such behaviors exemplify how the enhancement of magnetic frustration through NNN hopping inhibits the formation of stripes and promotes the emergence of superconductivity.

Pairing order—The superconducting order can be characterized by the singlet pairing amplitude $\Delta_{\mathbf{r},\mathbf{s}} = \langle c_{\mathbf{r}\uparrow} c_{\mathbf{s}\downarrow} - c_{\mathbf{r}\downarrow} c_{\mathbf{s}\uparrow} \rangle$. Specifically, we focus on the NN singlet pairing. As illustrated in Figs. 1(e)–1(g), we observe finite singlet pairing orders for both U(1) and SU(2) ground states. However, the pairing amplitude (averaged over the supercell) of the SU(2) states can be substantially larger than that in the U(1) states throughout the entire doping range for positive t'/t, as presented in Fig. 1(d). This can be attributed to the fact that the SU(2) iPEPS is, by construction, a spin-singlet state. Indeed, the latter can be interpreted as a generalized version of the resonating valence bond state [90]. Therefore, the existence of d-wave pairing order is reminiscent of Anderson's original resonating valence bond proposal [91,92].

Moreover, we discover that the singlet pairing for positive t'/t can be considerably larger than that for negative t'/t. Intuitively, this could be perceived as pair formation being enhanced (reduced) by the constructive (destructive) interference between NN and NNN hopping at positive (negative) t'/t [93]. This is in line with prior findings in the extended t-J model [60–62,94] and Hubbard model [63] using density matrix renormalization group. Electronic structure analysis [68,69,95,96] suggests that positive (negative) t'/t corresponds to electron (hole) doped cuprates. Consequently, the numerics so far yield outcomes that are opposite to the experimental observations, where hole-doped cuprates exhibit stronger superconductivity. This emphasizes the necessity for further investigations regarding the appropriate parameter settings in the effective models [61,97,98].

Long-range order—Figure 3(a) displays the long-range spin-spin $S_{\mathbf{rs}} = \langle \mathbf{S}_\mathbf{r} \cdot \mathbf{S}_\mathbf{s} \rangle - \langle \mathbf{S}_\mathbf{r} \rangle \cdot \langle \mathbf{S}_\mathbf{s} \rangle$ and pair-pair $P_{\mathbf{rs}} = \langle \Delta^{\mathbf{y}}_\mathbf{r} \Delta^{\mathbf{y}}_\mathbf{s} \rangle - \langle \Delta^{\mathbf{y}}_\mathbf{r} \rangle \langle \Delta^{\mathbf{y}}_\mathbf{s} \rangle$ (where $\Delta^{\boldsymbol{\alpha}}_\mathbf{r} = \Delta_{\mathbf{r},\mathbf{r}+\boldsymbol{\alpha}}$ and $\boldsymbol{\alpha} = \mathbf{x}, \mathbf{y}$ is the horizontal or vertical unit vector) correlators for two specific ground states with U(1) or SU(2) symmetry for $t'/t > 0$. Figure 3(b) shows the corresponding correlation lengths. Our data indicate that all these correlators decay exponentially, and the correlation lengths never exceed two

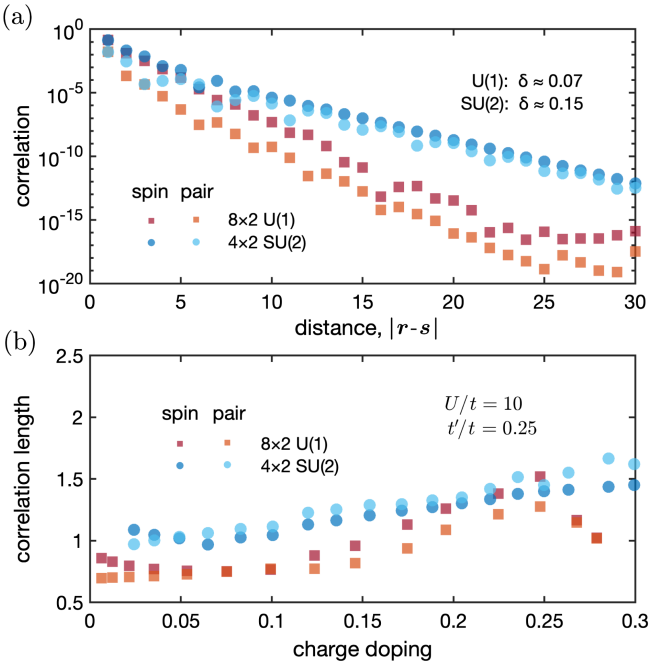

FIG. 3. (a) The long-range spin-spin and pair-pair correlators in the U(1) and SU(2) ground states, respectively. All these correlators exhibit an exponential decay behavior. (b) The corresponding correlation lengths as a function of doping.

units throughout the entire doping range. This suggests no connected long-range spin or pairing orders in both scenarios. Accordingly, a minor local pairing order sufficiently signals weak superconductivity in the stripe states.

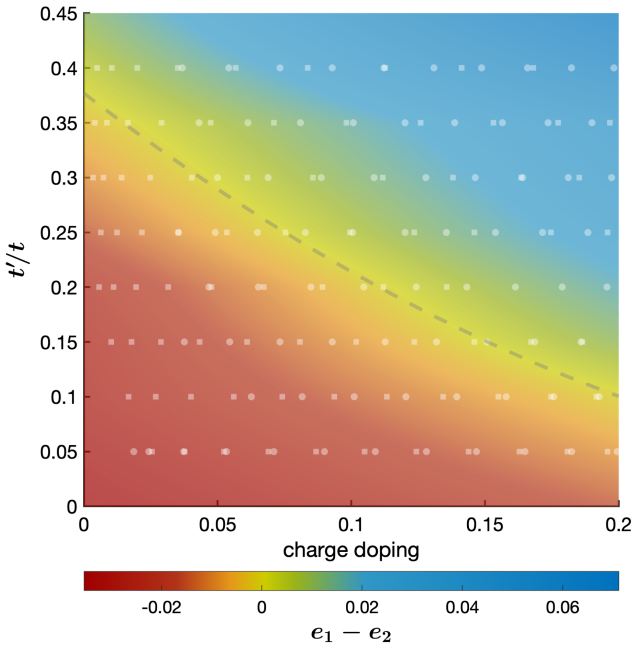

FIG. 4. The ground state phase diagram of the t-t' Hubbard model with respect to doping and t'/t. The color scale indicates $e_1 - e_2$, obtained via linear interpolation from a discrete set of scanning points (white). The gray dashed line marks $e_1 = e_2$.

Phase diagram—Figure 4 presents a schematic ground state *phase diagram* for $t'/t > 0$ derived via linear interpolation from a discrete set of scanning points. The U(1) stripe states are energetically favored in the bottom-left corner, and the SU(2) uniform states in the top-right corner. This is largely consistent with previous studies of the t-t'-J model [60]. Therefore, an increase of either charge doping or the NNN hopping, which both intensify magnetic frustration, will drive the ground state from striped to uniform states. Recall that the uniform ground states are typically accompanied by strong superconductivity. The phase diagram thus supports the conclusion that the enhancement of magnetic frustration helps stabilize superconductivity.

Discussion—In this research, we have studied the ground state properties and the phase diagram of the t-t' Hubbard model via the U(1) and SU(2) symmetric iPEPS method. We discovered an SU(2) uniform state with strong d-wave superconducting orders, with a lower energy than the striped U(1) states at large doping levels. Although the variational space of the U(1) iPEPS is larger than that of the SU(2) iPEPS, the fact that the U(1) iPEPS has so far failed to yield a uniform ground state suggests that the U(1) iPEPS has difficulty handling the subspace devoid of magnetic orders. This highlights the importance of exploring quantum states with several different global symmetries in tensor network simulations. We note, however, that it is possible to recover the SU(2) ground states via a U(1) implementation with *a priori* guidance about the SU(2) compatible settings; see Supplemental Material [78] for more details.

Also, we have demonstrated the interplay between local magnetic orders and superconductivity. The additional NNN interaction terms introduce extra magnetic frustration and help suppress the AFM orders, favoring strong d-wave superconductivity at large doping levels. Besides, a positive t'/t frustrates the domain walls and stimulates pair formation. This suggests that the superconductivity in cuprate materials can be enhanced, and T_c incremented, by elevating the strength of NNN hopping.

Outlook—The novel SU(2) ground state, expressed in terms of an iPEPS tensor network, contains information on dominant contributions from the many-body Hilbert space. Consequently, it is possible to generate various *snapshots* of the type accessible via quantum gas microscopy in the ultracold atom experiments [86,87], enabling a direct comparison with experimental analysis [89,99]. Such information would facilitate further investigations regarding the dopant mobility through high-order correlators [100,101] or string patterns using suitable pattern recognition algorithms [88]. Also, similar SU(2) symmetric tensor techniques can be applied to some thermal tensor network methods, such as finite temperature PEPS [102–104], exponential tensor renormalization group [99,105,106], or tangent space tensor renormalization group [107], to explore physics at finite temperatures where strange metal behavior is observed experimentally.

Acknowledgments—We thank our colleagues Andreas Weichselbaum and Andreas Gleis for stimulating discussions and technical suggestions, which led to a significant speedup of the algorithms. We also thank Philippe Corboz for helpful feedback on a preliminary version of this work, as well as Zi Yang Meng for constructive comments. This research was funded in part by the Deutsche Forschungsgemeinschaft under Germany's Excellence Strategy EXC-2111 (Project No. 390814868), and is part of the Munich Quantum Valley, supported by the Bavarian state government through the Hightech Agenda Bayern Plus.

[1] J. G. Bednorz and K. A. Müller, Z. Phys. B **64**, 189 (1986).
[2] B. Keimer, S. A. Kivelson, M. R. Norman, S. Uchida, and J. Zaanen, Nature (London) **518**, 179 (2015).
[3] P. A. Lee, N. Nagaosa, and X.-G. Wen, Rev. Mod. Phys. **78**, 17 (2006).
[4] J. Hubbard, Proc. R. Soc. A **296**, 82 (1967).
[5] S. R. White, Phys. Rev. Lett. **69**, 2863 (1992).
[6] R. Blankenbecler, D. J. Scalapino, and R. L. Sugar, Phys. Rev. D **24**, 2278 (1981).
[7] G. Sugiyama and S. Koonin, Ann. Phys. (N.Y.) **168**, 1 (1986).
[8] G. Knizia and Garnet Kin-Lic Chan, Phys. Rev. Lett. **109**, 186404 (2012).
[9] F. Verstraete and J. I. Cirac, arXiv:cond-mat/0407066.
[10] J. Jordan, R. Orús, G. Vidal, F. Verstraete, and J. I. Cirac, Phys. Rev. Lett. **101**, 250602 (2008).
[11] B.-X. Zheng, C.-M. Chung, P. Corboz, G. Ehlers, M.-P. Qin, R. M. Noack, H. Shi, S. R. White, S. Zhang, and G. K.-L. Chan, Science **358**, 1155 (2017).
[12] J. P. F. LeBlanc *et al.*, Phys. Rev. X **5**, 041041 (2015).
[13] J. M. Tranquada, B. J. Sternlieb, J. D. Axe, Y. Nakamura, and S. Uchida, Nature (London) **375**, 561 (1995).
[14] J. M. Tranquada, J. D. Axe, N. Ichikawa, Y. Nakamura, S. Uchida, and B. Nachumi, Phys. Rev. B **54**, 7489 (1996).
[15] R. J. Birgeneau, C. Stock, J. M. Tranquada, and K. Yamada, J. Phys. Soc. Jpn. **75**, 111003 (2006).
[16] G. Ghiringhelli *et al.*, Science **337**, 821 (2012).
[17] R. Comin and A. Damascelli, Annu. Rev. Condens. Matter Phys. **7**, 1 (2015).
[18] T. Wu, H. Mayaffre, S. Krämer, M. Horvatić, C. Berthier, W. N. Hardy, R. Liang, D. A. Bonn, and M.-H. Julien, Nature (London) **477**, 191 (2011).
[19] T. Wu, H. Mayaffre, S. Krämer, M. Horvatić, C. Berthier, W. Hardy, R. Liang, D. Bonn, and M.-H. Julien, Nat. Commun. **6**, 6438 (2015).
[20] A. Mesaros, K. Fujita, S. D. Edkins, M. H. Hamidian, H. Eisaki, S.-i. Uchida, J. C. S. Davis, M. J. Lawler, and E.-A. Kim, Proc. Natl. Acad. Sci. U.S.A. **113**, 12661 (2016).
[21] T. Giamarchi and C. Lhuillier, Phys. Rev. B **43**, 12943 (1991).
[22] E. Dagotto, Rev. Mod. Phys. **66**, 763 (1994).

[23] C. J. Halboth and W. Metzner, Phys. Rev. Lett. **85**, 5162 (2000).
[24] T. A. Maier, M. Jarrell, T. C. Schulthess, P. R. C. Kent, and J. B. White, Phys. Rev. Lett. **95**, 237001 (2005).
[25] M. Capone and G. Kotliar, Phys. Rev. B **74**, 054513 (2006).
[26] D. Eichenberger and D. Baeriswyl, Phys. Rev. B **76**, 180504(R) (2007).
[27] M. Aichhorn, E. Arrigoni, M. Potthoff, and W. Hanke, Phys. Rev. B **76**, 224509 (2007).
[28] L. F. Tocchio, F. Becca, A. Parola, and S. Sorella, Phys. Rev. B **78**, 041101(R) (2008).
[29] S. S. Kancharla, B. Kyung, D. Sénéchal, M. Civelli, M. Capone, G. Kotliar, and A.-M. S. Tremblay, Phys. Rev. B **77**, 184516 (2008).
[30] G. Sordi, P. Sémon, K. Haule, and A. M. S. Tremblay, Phys. Rev. Lett. **108**, 216401 (2012).
[31] E. Gull and A. J. Millis, Phys. Rev. B **86**, 241106(R) (2012).
[32] H. Yokoyama, M. Ogata, Y. Tanaka, K. Kobayashi, and H. Tsuchiura, J. Phys. Soc. Jpn. **82**, 014707 (2012).
[33] J. Kaczmarczyk, J. Spałek, T. Schickling, and J. Bünemann, Phys. Rev. B **88**, 115127 (2013).
[34] E. Gull, O. Parcollet, and A. J. Millis, Phys. Rev. Lett. **110**, 216405 (2013).
[35] K.-S. Chen, Z. Y. Meng, S.-X. Yang, T. Pruschke, J. Moreno, and M. Jarrell, Phys. Rev. B **88**, 245110 (2013).
[36] J. Otsuki, H. Hafermann, and A. I. Lichtenstein, Phys. Rev. B **90**, 235132 (2014).
[37] Y. Deng, E. Kozik, N. V. Prokof'ev, and B. V. Svistunov, Europhys. Lett. **110**, 57001 (2015).
[38] L. F. Tocchio, F. Becca, and S. Sorella, Phys. Rev. B **94**, 195126 (2016).
[39] D. Poilblanc and T. M. Rice, Phys. Rev. B **39**, 9749 (1989).
[40] J. Zaanen and O. Gunnarsson, Phys. Rev. B **40**, 7391 (1989).
[41] S. R. White and D. J. Scalapino, Phys. Rev. Lett. **91**, 136403 (2003).
[42] G. Hager, G. Wellein, E. Jeckelmann, and H. Fehske, Phys. Rev. B **71**, 075108 (2005).
[43] C.-C. Chang and S. Zhang, Phys. Rev. Lett. **104**, 116402 (2010).
[44] H.-H. Zhao, K. Ido, S. Morita, and M. Imada, Phys. Rev. B **96**, 085103 (2017).
[45] E. W. Huang, C. B. Mendl, H.-C. Jiang, B. Moritz, and T. P. Devereaux, npj Quantum Mater. **3**, 22 (2018).
[46] A. S. Darmawan, Y. Nomura, Y. Yamaji, and M. Imada, Phys. Rev. B **98**, 205132 (2018).
[47] T. I. Vanhala and P. Törmä, Phys. Rev. B **97**, 075112 (2018).
[48] K. Ido, T. Ohgoe, and M. Imada, Phys. Rev. B **97**, 045138 (2018).
[49] K. Machida, Physica (Amsterdam) **158C**, 192 (1989).
[50] M. Kato, K. Machida, H. Nakanishi, and M. Fujita, J. Phys. Soc. Jpn. **59**, 1047 (1990).
[51] B. Ponsioen, S. S. Chung, and P. Corboz, Phys. Rev. B **100**, 195141 (2019).
[52] L. F. Tocchio, A. Montorsi, and F. Becca, SciPost Phys. **7**, 021 (2019).
[53] J. M. Tranquada, J. D. Axe, N. Ichikawa, A. R. Moodenbaugh, Y. Nakamura, and S. Uchida, Phys. Rev. Lett. **78**, 338 (1997).
[54] R. Eder, Y. Ohta, and G. A. Sawatzky, Phys. Rev. B **55**, R3414 (1997).
[55] G. B. Martins, R. Eder, and E. Dagotto, Phys. Rev. B **60**, R3716 (1999).
[56] H.-C. Jiang and T. P. Devereaux, Science **365**, 1424 (2019).
[57] B.-X. Zheng and Garnet Kin-Lic Chan, Phys. Rev. B **93**, 035126 (2016).
[58] C.-M. Chung, M. Qin, S. Zhang, U. Schollwöck, and S. R. White, Phys. Rev. B **102**, 041106(R) (2020).
[59] Y.-F. Jiang, J. Zaanen, T. P. Devereaux, and H.-C. Jiang, Phys. Rev. Res. **2**, 033073 (2020).
[60] S. Gong, W. Zhu, and D. N. Sheng, Phys. Rev. Lett. **127**, 097003 (2021).
[61] S. Jiang, D. J. Scalapino, and S. R. White, Proc. Natl. Acad. Sci. U.S.A. **118**, e2109978118 (2021).
[62] S. Jiang, D. J. Scalapino, and S. R. White, Phys. Rev. B **106**, 174507 (2022).
[63] Y.-F. Jiang, T. P. Devereaux, and H.-C. Jiang, arXiv:2303.15541.
[64] H. Xu, C.-M. Chung, M. Qin, U. Schollwöck, S. R. White, and S. Zhang, Science **384**, adh7691 (2024).
[65] H. C. Jiang, Z. Y. Weng, and T. Xiang, Phys. Rev. Lett. **101**, 090603 (2008).
[66] A. Weichselbaum, Ann. Phys. (Amsterdam) **327**, 2972 (2012).
[67] A. Weichselbaum, Phys. Rev. Res. **2**, 023385 (2020).
[68] M. Hirayama, Y. Yamaji, T. Misawa, and M. Imada, Phys. Rev. B **98**, 134501 (2018).
[69] M. Hirayama, T. Misawa, T. Ohgoe, Y. Yamaji, and M. Imada, Phys. Rev. B **99**, 245155 (2019).
[70] P. Corboz, R. Orús, B. Bauer, and G. Vidal, Phys. Rev. B **81**, 165104 (2010).
[71] P. Corboz, J. Jordan, and G. Vidal, Phys. Rev. B **82**, 245119 (2010).
[72] B. Bruognolo, J.-W. Li, J. von Delft, and A. Weichselbaum, SciPost Phys. Lect. Notes **25** (2021).
[73] C. V. Kraus, N. Schuch, F. Verstraete, and J. I. Cirac, Phys. Rev. A **81**, 052338 (2010).
[74] T. Barthel, C. Pineda, and J. Eisert, Phys. Rev. A **80**, 042333 (2009).
[75] F. Verstraete, V. Murg, and J. Cirac, Adv. Phys. **57**, 143 (2008).
[76] P. Corboz, Phys. Rev. B **93**, 045116 (2016).
[77] H.-J. Liao, J.-G. Liu, L. Wang, and T. Xiang, Phys. Rev. X **9**, 031041 (2019).
[78] See Supplemental Material at http://link.aps.org/supplemental/10.1103/PhysRevLett.134.116502 for technical details and additional numerical results.
[79] G. Vidal, Phys. Rev. Lett. **98**, 070201 (2007).
[80] P. Corboz, S. R. White, G. Vidal, and M. Troyer, Phys. Rev. B **84**, 041108(R) (2011).
[81] T. Nishino and K. Okunishi, J. Phys. Soc. Jpn. **65**, 891 (1996).
[82] P. Corboz, T. M. Rice, and M. Troyer, Phys. Rev. Lett. **113**, 046402 (2014).
[83] R. Orús and G. Vidal, Phys. Rev. B **80**, 094403 (2009).

[84] A. Weichselbaum, Open Source QSpace 4.0.
[85] J. Koepsell, D. Bourgund, P. Sompet, S. Hirthe, A. Bohrdt, Y. Wang, F. Grusdt, E. Demler, G. Salomon, C. Gross, and I. Bloch, Science **374**, 82 (2021).
[86] J. Koepsell, J. Vijayan, P. Sompet, F. Grusdt, T. A. Hilker, E. Demler, G. Salomon, I. Bloch, and C. Gross, Nature (London) **572**, 358 (2019).
[87] J. Koepsell, S. Hirthe, D. Bourgund, P. Sompet, J. Vijayan, G. Salomon, C. Gross, and I. Bloch, Phys. Rev. Lett. **125**, 010403 (2020).
[88] C. S. Chiu, G. Ji, A. Bohrdt, M. Xu, M. Knap, E. Demler, F. Grusdt, M. Greiner, and D. Greif, Science **365**, 251 (2019).
[89] B.-B. Chen, C. Chen, Z. Chen, J. Cui, Y. Zhai, A. Weichselbaum, J. von Delft, Z. Y. Meng, and W. Li, Phys. Rev. B **103**, L041107 (2021).
[90] J.-W. Li, B. Bruognolo, A. Weichselbaum, and J. von Delft, Phys. Rev. B **103**, 075127 (2021).
[91] G. Baskaran, Z. Zou, and P. Anderson, Solid State Commun. **63**, 973 (1987).
[92] P. W. Anderson, G. Baskaran, Z. Zou, and T. Hsu, Phys. Rev. Lett. **58**, 2790 (1987).
[93] G. B. Martins, J. C. Xavier, L. Arrachea, and E. Dagotto, Phys. Rev. B **64**, 180513(R) (2001).
[94] X. Lu, F. Chen, W. Zhu, D. N. Sheng, and S.-S. Gong, Phys. Rev. Lett. **132**, 066002 (2024).
[95] T. Tohyama and S. Maekawa, Phys. Rev. B **49**, 3596 (1994).
[96] O. Andersen, A. Liechtenstein, O. Jepsen, and F. Paulsen, J. Phys. Chem. Solids **56**, 1573 (1995).
[97] T. Xiang, H. G. Luo, D. H. Lu, K. M. Shen, and Z. X. Shen, Phys. Rev. B **79**, 014524 (2009).
[98] S. Jiang, D. J. Scalapino, and S. R. White, Phys. Rev. B **108**, L161111 (2023).
[99] D.-W. Qu, B.-B. Chen, X. Lu, Q. Li, Y. Qi, S.-S. Gong, W. Li, and G. Su, Phys. Rev. Lett. **133**, 256003 (2024).
[100] A. Bohrdt, Y. Wang, J. Koepsell, M. Kánasz-Nagy, E. Demler, and F. Grusdt, Phys. Rev. Lett. **126**, 026401 (2021).
[101] C. Hubig, A. Bohrdt, M. Knap, F. Grusdt, and I. Cirac, SciPost Phys. **8**, 021 (2020).
[102] P. Czarnik, L. Cincio, and J. Dziarmaga, Phys. Rev. B **86**, 245101 (2012).
[103] P. Czarnik and J. Dziarmaga, Phys. Rev. B **90**, 035144 (2014).
[104] P. Czarnik and J. Dziarmaga, Phys. Rev. B **92**, 035152 (2015).
[105] B.-B. Chen, L. Chen, Z. Chen, W. Li, and A. Weichselbaum, Phys. Rev. X **8**, 031082 (2018).
[106] H. Li, B.-B. Chen, Z. Chen, J. von Delft, A. Weichselbaum, and W. Li, Phys. Rev. B **100**, 045110 (2019).
[107] Q. Li, Y. Gao, Y.-Y. He, Y. Qi, B.-B. Chen, and W. Li, Phys. Rev. Lett. **130**, 226502 (2023).